16th World Conference on Earthquake, 16WCEE 2017

Santiago Chile, January 9th to 13th 2017

Paper N° 1226

Registration Code: S-K1464692894

ANALYSIS ON DAMAGE OF THE EXISTING SEISMIC ISOLATION BRIDGE DUE TO THE 2011 GREAT EAST JAPAN EARTHQUAKE

R. Fujita[(1)], M. Sadamatsu[(2)], Y. Takahashi[(3)]

[(1)] *Project Manager, Eight-Japan Engineering Consultants, Inc., fujita-ryo@ej-hds.co.jp*
[(2)] *Engineer, Eight-Japan Engineering Consultants, Inc., sadamatsu-ma@ej-hds.co.jp*
[(3)] *Associate Professor, Graduate School of Engineering, Kyoto University, takahashi.yoshisuke.4v@kyoto-u.ac.jp*

Abstract

Due to the 2011 Great East Japan Earthquake, some seismic isolation bridges were severely damaged by ground motion and cracks of isolation bearings were observed. In this paper, one of the damaged bridges was picked and dynamic analyses were conducted to clarify the cause of damage of the bridge. As a result of the reproduction analyses of the bridge using the estimated ground motion based on aftershock observations, it is estimated that the isolation bearings were damaged by shearing and vertical force due to rocking vibration of the superstructure.

Keywords: seismic isolation bridge; seismic damage; rubber bearing; reproduction analysis; 2011 Great East Japan Earthquake

1. Outline

When the 2011 Great East Japan Earthquake struck, damage to the bearing section of some bridges using rubber bearings was reported. [1] Reproduction analysis using the dynamic analysis technique was conducted for this paper for a seismic isolation bridge selected from among bridges which had suffered such damage to analyze the causes of damage. The findings of this analysis are described below.

2. Specifications of the Subject Bridge and Outline of Damage

The subject bridge is 981.2 m long and 8.250 m wide (main lines) with 18 spans (continuous PC girder for 7 spans x 2 (main line section) and continuous PC girder for 4 spans (ramp bridge section)). The substructure consists of a body made up of RC oval piers, rigid frame abutments and reversed T type abutments and the foundations consist of spread foundations (As1 abutment to P4 pier), steel pipe steel pile foundations (P5 to P14 piers) and pile foundations (A2 abutment). The bearings are layered rubber bearings containing lead plugs. The applicable standard is the 1996 Specifications for Highway Bridges. [2] A general drawing of the pier and a plan of the subject bridge are shown in Fig. 1 and Fig. 2 respectively.

Although the pier and girders of the subject bridge were not damaged, the seismic isolation bearings suffered cracks to the sides of the bearings and interference between the cladding rubber for corrosion prevention and the side blocks. A 41 cm long horizontal crack occurred with the seaward side G1 bearings among three seismic isolation bearings (layered rubber bearings containing round lead plugs) situated on one bearing line above the As1 abutment of the ramp bridge section. Details of the crack are shown in Fig. 3.

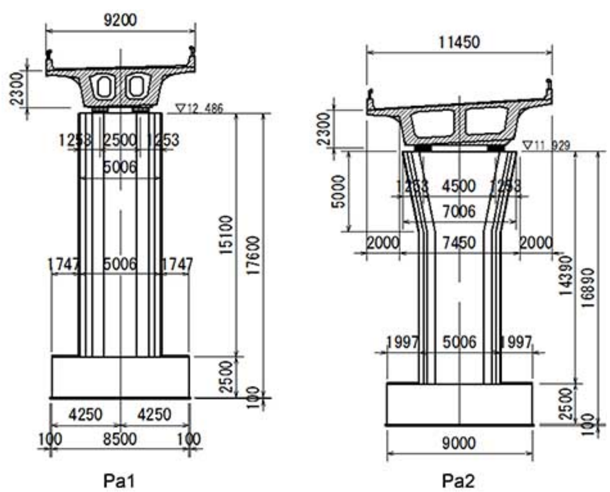

Fig. 1 General drawing of the pier

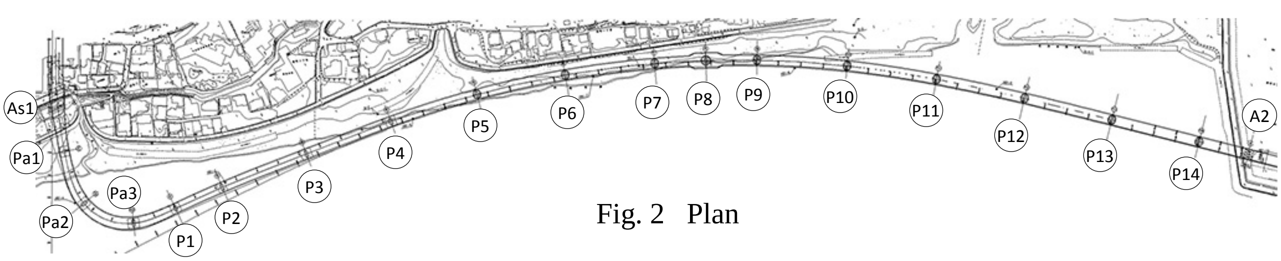

Fig. 2 Plan

Needle pricked to check the crack depth

Fig. 3 Crack on G1 bearing of As1 abutment

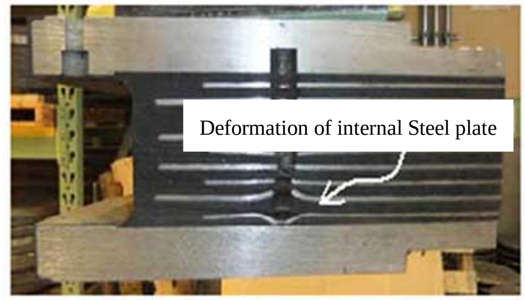

(a) Deformation of internal steel plate around the positioning hole

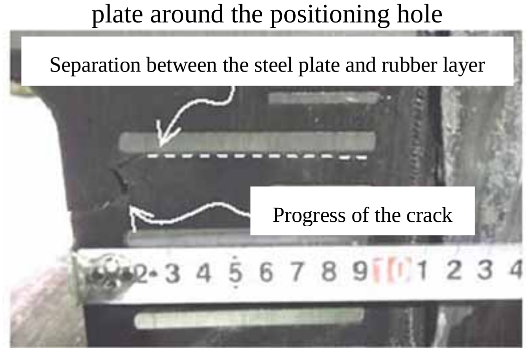

(b) Travelling direction of the crack

Fig. 4 Cross-section of G1 bearing of As1 abutment

3. Observation Records in the Surrounding Area and Estimated Seismic Wave

There are several seismic waveform observation stations within a 5 km radius from this elevation bridge. These are the K-NET Hitachi (IBR003), NEXCO Hitachi-North IC and MLIT Hitachi Observation Stations. As seismic records from these sites have the characteristic of showing a sudden drop in the response spectrum when the natural period increased above 0.8 seconds (Figs. 5 and 6), they may not properly indicate damage to a seismic isolation bridge. In their observation of after-shocks, Hata, et al. [3] confirmed highly significant discrepancies in terms of the form of H/V spectra and peak frequencies between the K-NET Hitachi Station and the subject bridge site, pointing out the likelihood that the site characteristics greatly change near the subject bridge site. They also estimated seismic motion based on the evaluation results of the site characteristics though after-shock observation using the site characteristics replacement method. The estimated seismic motion exceeds the Type I seismic motion spectrum and is nearly equivalent to the Type II seismic motion spectrum. In some areas, the acceleration response spectrum is found to be slightly above the Type II spectrum.

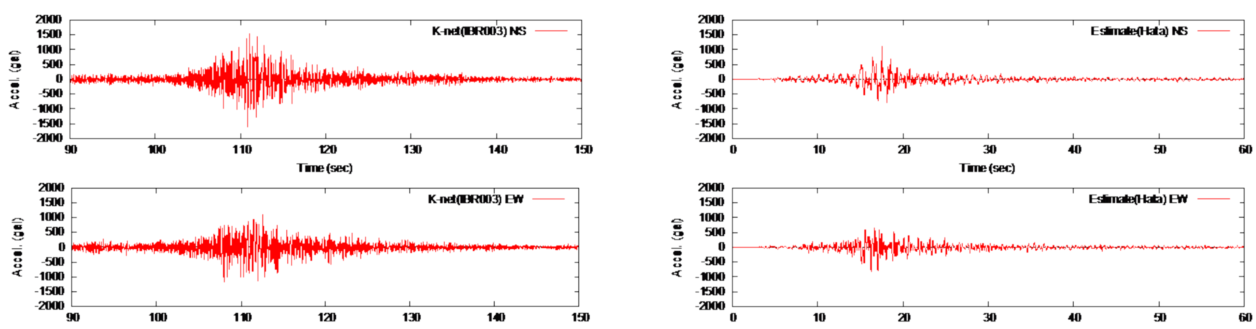

(a) Recorded wave (K-NET IBR003) (b) Estimated wave

Fig. 5 Observation records for the surrounding area and accelerogram of the estimated wave

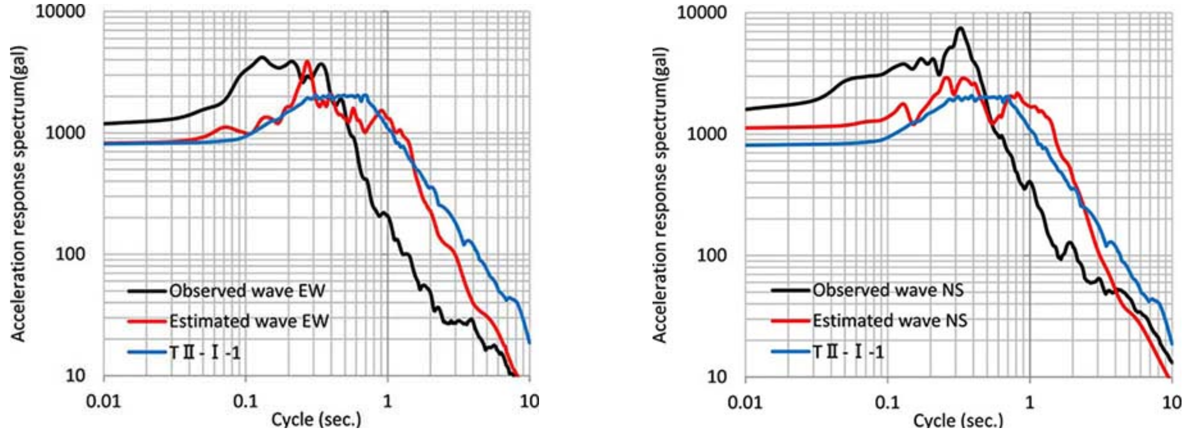

(a) E-W direction component (b) N-S direction component

Fig. 6 Observation records for the surrounding area and acceleration response spectrum of the estimated wave

4. Analytical Model

The ramp bridge section having experienced a major crack is a curved bridge while the side blocks of the bearings in the main lines section were also damaged. Under these circumstances, a dynamic analysis was conducted with a model corresponding to the entire structure, including the main lines section where the side blocks of the bearings were damaged. The analytical model is shown in Fig. 7. The modelling of the piers was based on the beam elements, taking the non-linearity of the bending into consideration, and the non-linear characteristics were calculated in accordance with the 1996 Specifications for Highway Bridges (Table 1). The modelling of the seismic isolation bearings was based on the positioning of the non-linear spring (bi-linear model) at the site of each bearing. The design displacement (response displacement to Level 2 seismic motion in the 1996 Specification for Highway Bridges) of the bearings and the corresponding equivalent stiffness, flat dimensions and total rubber thickness are shown in Table 1.

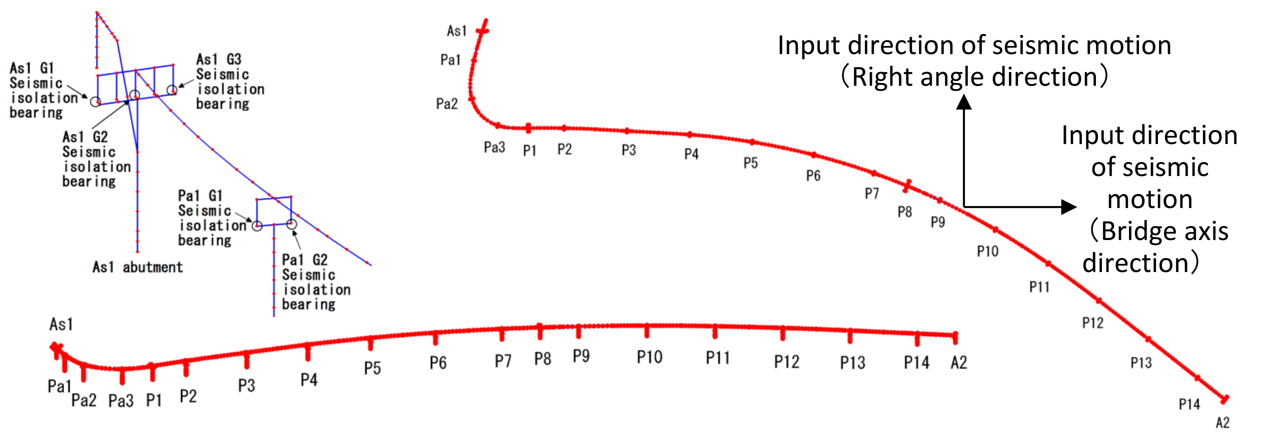

Fig. 7 Analytical model (bottom left: bird’s eye view; top right: plan; top left: details of the bearing section)

Table 1 Specifications of the bearings (ramp bridge section)

	Design displacement	Equivalent stiffness	Flat dimension	Total rubber thickness
	mm	kN/mm	mm	mm
As1	203	4	ϕ720	110
Pa1	128	12	ϕ1120	99
Pa2	142	15	ϕ1170	87
Pa3	161	14	ϕ1170	93
P1(Pa3 side)	158	4	ϕ720	108

The analysis conditions are shown in Table 2. The damping constant for the members was determined with reference to the Specifications for Highway Bridges. The Rayleigh damping constant was determined to represent the principal mode after the damping constant for each model was calculated based on the eigenvalue analysis results in accordance with the principle of proportional damping to strain energy. The natural vibration modes are shown in Figs. 8 and 9 (the equivalent stiffness was used for the seismic isolation bearing sections).

Table 2 Analysis conditions

Item			Set Conditions
Conditions of dynamic analysis	Solution to equation of motion		Direct integral method
	Numerical integration		Newmark-β method (β=1/4)
	Integration interval		0.01 sec. (Automatic detail analysis when convergence 0.02 conditions are not met)
	Damping matrix		Setting-up of Rayleigh damping based on the eigenvalue analysis results
	Non-linear analysis		Unbalanced force is added to the next step as residual load
	Definition of stiffness of non-linear element		Non-linear judgement using the averaged moment at the ends of beam elements
Structural conditions	Model		Space frame model
	Modeling of members	Superstructure	Linear beam element
		Pier	Non-linear beam element
		Seismic isolation bearing	Non-linear spring element
	Modeling of weight	Superstructure	Nodal point weight
		Pier	Nodal point weight
		Footing	Nodal point weight
	Damping constant of members	Superstructure	3%
		Bearing	0%
		Pier	2%
		Foundations	10% (Type I ground)
		Rigid member	0%
	Non-linear characteristics of members	Superstructure	–
		Bearing	Bilinear model
		Pier	Trilinear type skeleton curve (Takeda model)

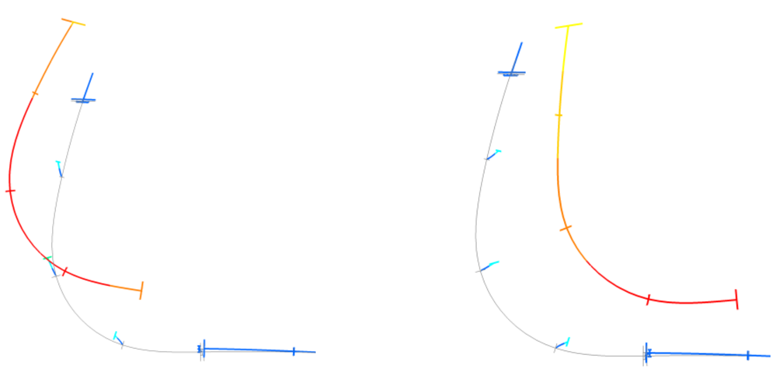

Primary mode (1.45 sec.) Secondary mode (1.44 sec.)

Fig. 8 Natural vibration model for the ramp section

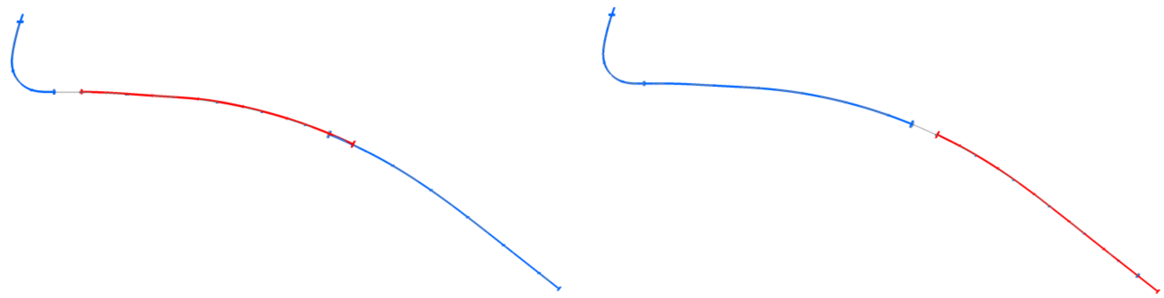

Primary mode (1.62 sec.) Secondary mode (1.59 sec.)

Fig. 9 Natural vibration mode for the main lines section

5. Analysis Focusing on Damage to Seismic Isolation Bearings at the Ramp Section

5.1 Outline of Analysis

The main damage to the seismic isolation bearings was a crack at the G1 bearing at the As1 abutment (hereinafter referred to as the As1 bearing, G1 bearings at the Pa2, Pa3 and P1 piers are similarly referred to as Pa2, Pa3 and P1 bearings respectively). As shown earlier, a trapezoidal crack occurred at the As1 bearing, suggesting that the bearing had fractured due to shearing deformation. Some minor cracks also occurred with the P1 bearing (the ending point side) and P8 bearing. For the purpose of the present analysis, the As1 bearing with a prominent crack was selected for dynamic analysis for reproduction of the crack to infer the causes of damage. While the basic analysis conditions were those commonly used for the investigation of the aseismic performance of road bridges, a comparative analysis was conducted focusing on the following conditions and response values thought to affect the behavior of the bridge at the time of the earthquake.

① Input seismic motion

② Vertical force acting on the bearing

The results of this comparative analysis are described in detail next.

5.2 Results of Calculations Focusing on Input Seismic Motions

The input seismic motions used for the dynamic analysis were the observed wave at the K-NET Hitachi station (observed wave), the estimated wave based on the after-shock observation results (estimated wave) and the acceleration waveform II-I-1 given in the Specifications for Highway Bridges Part 5 Seismic Design (Specifications wave). The Specifications wave was input in a single direction along the bridge axis (north-south) and at a right angle (east-west). The observed wave and estimated wave were input in two horizontal directions (see Fig. 7; no input in the vertical direction is made).

Figs. 10 to 12 show the response results of the As1 bearing. The displacement of each bearing along the tangential direction to the road axis is shown as that in the bridge axis direction. The perpendicular displacement to the bridge axis direction is shown as that in the right angle direction. The maximum response displacement of the seismic isolation bearing caused by the observed seismic motion was 54 mm in the bridge axis direction and 88 mm in the right angle direction, equivalent to some 30% of the allowable displacement of 275 mm (displacement at 250% strain). In an experiment [4] by Shinohara et al., the removed seismic isolation bearing (G2 bearing of the As1 abutment) produced a stable history with repetitive loading at a 250% shearing strain. As the rupture strain was 276%, it is unlikely that the observed seismic motion would cause cracking or other deformation to the bearings. When the Specifications wave was input, the bearing showed a response at some

80% of the allowable displacement. In the case of the estimated wave, the response was approximately 1.5 times the allowable displacement.

Fig. 13 shows the ratio between the allowable displacement of the bearings and the maximum response values. Figs. The analysis results of the input estimated wave show excess displacement of some 50% above the design allowable value in the bridge axis direction for the As1 bearing (shearing strain of 367%). The allowable value is exceeded in the case of other bearings on the piers in either the bridge axis or right angle direction. While the displacement of the As1 bearing is large as an absolute value of displacement, the excess ratio above the allowable value is large for every bearing in the ramp section. This means that the damage to the As1 bearing cannot be described as being excessively severe compared to other bearings.

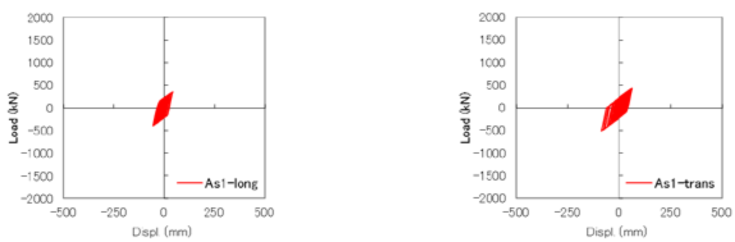

(Bridge axis) (Right angle)

Fig. 10 Load on the As1 bearing: displacement history (observed wave)

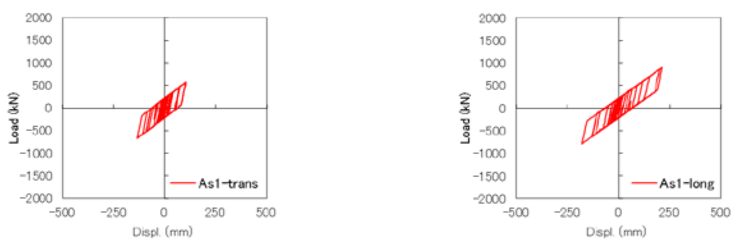

(Bridge axis) (Right angle))

Fig. 11 Load on As1 bearing: displacement history (Specifications wave)

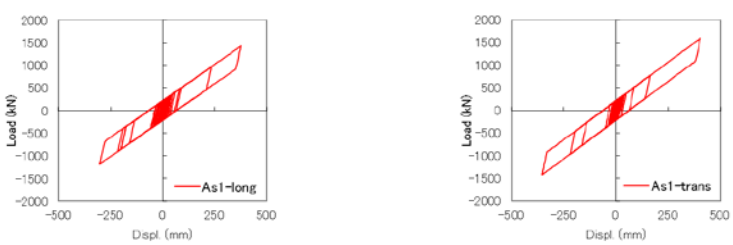

(Bridge axis) (Right angle)

Fig. 12 Load on As1 bearing: displacement history (estimated wave)

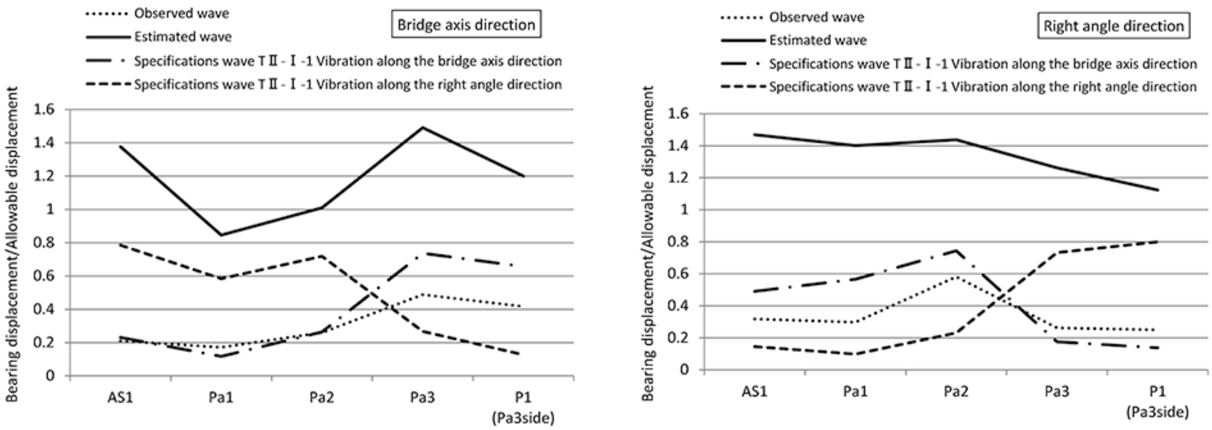

Fig. 13 Ratio between the displacement of the seismic isolation bearing and allowable displacement

The response history of the pier in Fig. 14 shows a minor yield of the P1 pier in the bridge axis direction while a significant non-linear response is shown for the P8 pier. These analysis results are not compatible with the damage survey results where damage to the piers by the earthquake was not found.

As the estimated wave is the only seismic motion where the displacement of the bearing exceeds the allowable value, it is safe to assume that, compared to the observed wave, the estimated wave represents the seismic motion which would have occurred at the point in question to a certain extent. Accordingly, use of the estimated wave is judged to be suitable to reproduce the actual seismic damage and this is used as the seismic motion for input in the calculations in the following sections.

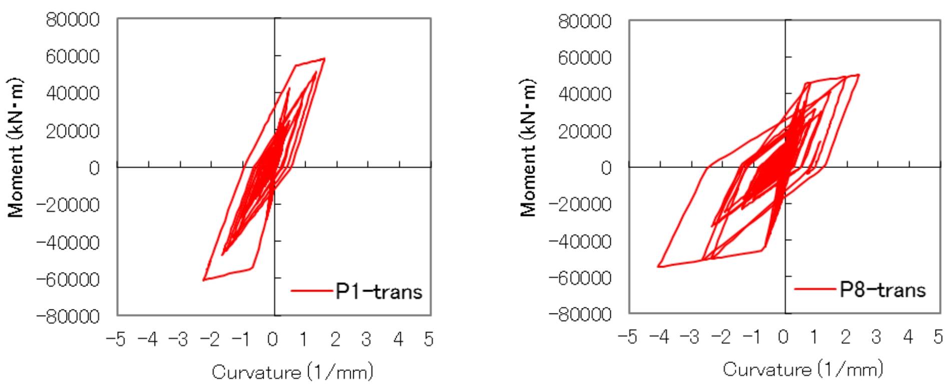

(P1 Right angle) (P8 Right angle)

Fig. 14 Pier response under the input of the estimated wave

5.3 Results of Calculations Focusing on the Vertical Force Acting on the Bearings

5.3.1 Analysis focusing on the tensile stress

The trial calculations confirmed that none of the matters focused on so far were principal causes of the concentrated damage to the As1 bearing, indicating that the horizontal response of the bearing alone cannot fully express the actual phenomenon.

The maximum response values of the bearings were then recalculated focusing on their behavior in not only the horizontal direction but also the vertical direction (vertical tensile force at the bearing as a result of the rocking vibration of the girder around the bridge axis). Tensile force was generated at the As1 and P1 bearings and the value of this tensile force at the As1 bearing was approximately double the design allowable tensile stress of 2N/mm^2. As the dead weight tends to be smaller at the end section of the continuous girder compared to the middle section, the area of the bearing tends to be small. The small resistance at these releasing ends to the girder twist likely means large vertical tensile stress at the bearings located at the girder end section.

The time history of the vertical force acting on the As1 bearing (Fig. 15) shows an anti-phase between the vertical force acting on the G1 and G3 bearings, suggesting the generation of large vertical force caused by rocking of the girder in the right angle direction on the end section bearings. In regard to the As1 bearing, three bearings are actually installed on a single bearing line and these three bearings share the dead load reaction force to slightly different degrees. The two end bearings (As1 G1 and As1 G3) share the force caused by girder rotation at the time of an earthquake. The time history clearly shows that the maximum vertical tensile force at the central G2 bearing is smaller than that at the G1 and G3 bearings. As the cross-sectional area of a bearing is often determined against the dead load reaction force, a larger number of bearings on a single bearing line means a smaller cross-sectional area of individual bearings. Because of this, the cross-sectional area of the bearings at As1 is smaller than that of the bearings at other piers where two bearings are installed per single bearing line, resulting in large tensile stress against the same vertical force.

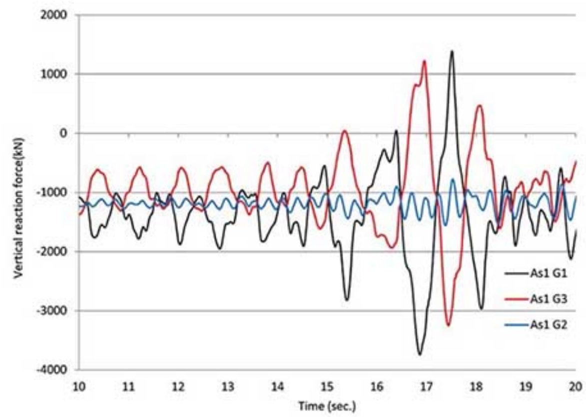

Fig. 15 Time history of vertical reaction force at the seismic isolation bearing (forward tension)

5.3.2 Analysis focusing on the effective area of the bearings

The next subject for analysis is the results of the analysis focusing on the effective tension area of the bearings (area of rubber bearing the tensile force where the horizontal moving amount is deducted). An experiment [5] confirmed that a smaller effective tension area due to a larger shearing deformation of a bearing decreases the rupture tensile force and that the rupture stress taking the effective tensile area into consideration is around 5 N/mm^2 even though it is not necessarily uniform. The calculation results for 10 seconds through 20 seconds where the response value is large are examined from this viewpoint. Fig. 21 shows the calculation results for the effective tension area based on the displacement history of the As1 bearing shown in Figs. 19 and 20. It is shown that the effective tension area is small at around 16 seconds, 17 seconds and 17.5 seconds where the horizontal displacement of the bearing is large. Fig. 19 shows the calculated vertical stress based on these results and the vertical reaction force (Fig. 15). Both the tensile stress of the G3 bearing of around 17 seconds and the tensile stress of the G1 bearing of around 17.5 seconds where the effective area is small exceed the rupture strength of 5N/mm^2. At these times, a large tensile force acts on each bearing and it may be the case that the acting of a large tensile force on bearings experiencing major horizontal displacement leads to rupture of the rubber.

The displacement waveform confirmed that the displacement in the bridge axis direction was restrained to ± 300mm due to the structure limiting displacement and that collision occurred at around 16 seconds and 17 seconds. In the right angle direction, axis direction was restrained to ± 200mm and collision occurred at around 17 seconds and 17.5 seconds. Compared to the case where the structure to limit displacement is ignored, the displacement of the bearing is smaller, reducing the amount of decrease of the effective tension area but the vertical force becomes larger. In short, the vertical stress acting on the bearing becomes larger.

Based on the above calculation results, the tensile stress caused by the vertical force acting on the bearing is thought to have exceeded the rupture strength, constituting one cause of the damage to the As1 bearing.

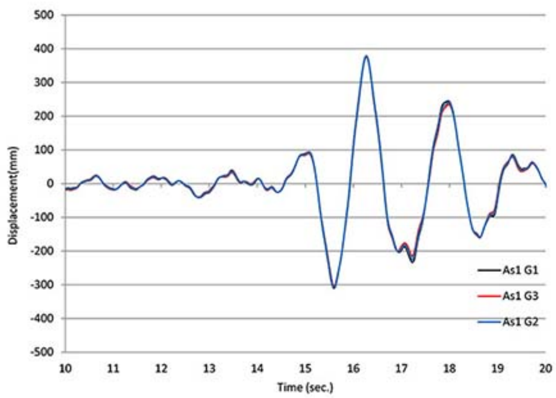

Fig. 16 Displacement history in the bridge axis direction at the As1 bearing

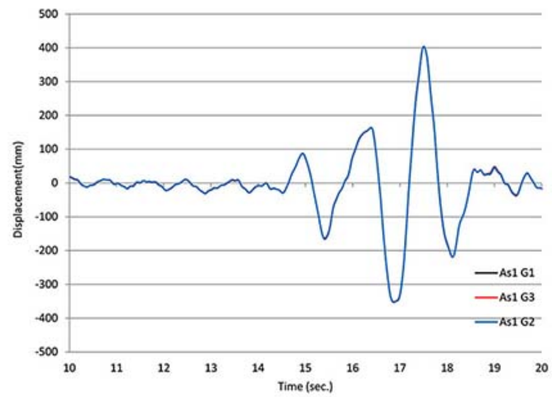

Fig. 17 Displacement history in the right angle direction at the As1 bearing

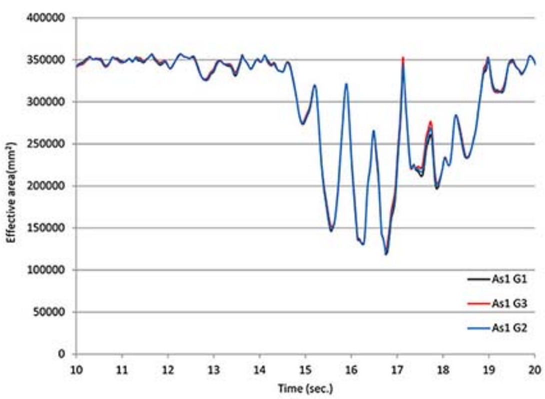

Fig. 18 Time history of effective tensile area at the As1 bearing

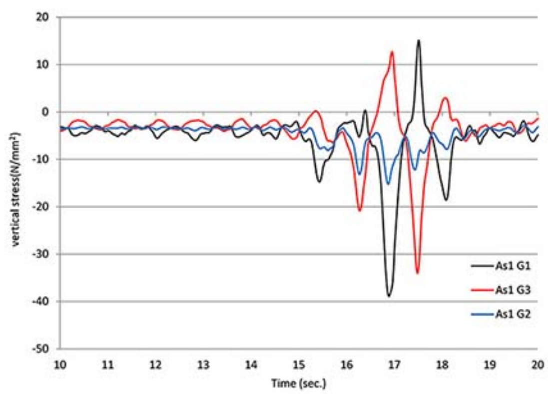

Fig. 19 Time history of vertical stress at the As1 bearing (forward tension)

6. Conclusions

This study has attempted to reproduce the situation of damage using dynamic analysis featuring an existing seismic isolation bridge of which the bearings were damaged by the 2011 Great East Japan Earthquake. The knowledge obtained from a series of analyses is explained here.

① The response value of the bridge is small when observed data near the bridge site is used. In a calculation using the estimated wave incorporating the impacts of the surrounding ground, the horizontal displacement of a bearing exceeds the allowable displacement. The calculation results using the estimated wave are more compatible with the state of the actual damage, indicating the possibility that a larger seismic motion than that observed at nearby observation sites occurred at the subject bridge site.

② The results of the dynamic analysis indicate that shearing deformation exceeding the allowable value occur with all of the bearings in the ramp section. This suggests that there is another cause of the concentrated damage to the As1 bearing.

③ It is thought that the horizontal response of the bearing alone cannot fully express the actual phenomenon and focus was placed on the tensile force in the vertical direction which is generated for the bearings as a result of rocking of the girder. It is found that large tensile stress is generated at the As1 bearing due to the large vertical force acting on it as well as a decrease of the effective tension area caused by horizontal deformation of the bearing. This large tensile stress is thought to have been the principal cause of the damage to the As1 bearing. This tensile force in the vertical direction is generated by girder rotation around the bridge axis. A larger number of bearings on a single bearing line tends to increase the load on the bearings at the ends and this is believed to explain the concentrated damage to the end bearings for the As1 abutment.

④ The inferred damage mechanism based on the state of the damage to the As1 bearing and the relevant calculation results suggest the following sequence leading to the actual damage.

- The vertical tensile force acts on the bearing of which the effective tension area has decreased due to horizontal deformation.
- The rubber and steel plate are separated inside the bearing.
- The horizontal deformation of the bearing progresses in a reverse direction and the force vertically acting on the bearing is reversed to increase the compaction force.
- The shearing deformation as a result of the slipping between the rubber and steel place inside the bearing reaches the bearing surface, creating a trapezoidal crack.
- The damage to the rubber loosens the lead plugs. These plugs then separate from the rubber and some of them flow out.

⑤ The analysis results this time do not show a significant difference in response between the G1 bearing and G3 bearing of the As1 abutment. In reality, however, the G1 bearing suffered significant damage. A possible reason for this is that the vertical tensile force at the time of an earthquake occurs more readily with the G1 bearing, making the G1 bearing more susceptible to damage because of the smaller initial vertical compaction force with the G1 bearing than the G3 bearing. In the model for the present analysis, the girders are assumed to be a single beam, failing to express the initial bias in load distribution. When a more detailed model of the girders is developed using a grid or plates, any difference between the G1 bearing and G3 bearing should be verified more accurately.

Based on a series of trial calculations focusing on several possible causes, one viable explanation for the rupture of the As1 bearing is believed to have been established. Needless to say, the actual behavior of a bridge at the time of an earthquake is much more complex due to many affecting elements and it is impossible to explain everything with one cause. Nevertheless, the present sensitivity analysis using the numerical analysis method indicates a likely candidate for the principal cause. The effectiveness of the seismic isolation bearing to improve the aseismic performance of a bridge is clear because of the limited damage to the subject bridge despite the strong possibility of major seismic force acting on the bridge during the featured earthquake. At the same time, the present analysis confirms the possibility of an unexpected concentration of load on the bearings as their motion is restricted by the surrounding members when a seismic isolation bridge is subjected to a greater seismic force than the design seismic force.

7. Acknowledgements

For the presentation of this paper, we were fortunate to be able to use the observation data of the K-NET of the National Research Institute for Earth Science and Disaster Prevention (NIED), the Ministry of Land, Infrastructure, Transport and Tourism (MLIT) and the East Nippon Expressway Co., Ltd. We also received many useful comments from members of the Subcommittee for Analysis of the Damage to Bridges, etc. by the Great East Japan Earthquake, Earthquake Engineering Committee, Japan Society of Civil Engineers. We would like to express our utmost gratitude to all organizations and individuals for their kind assistance.

8. References

[1] Takahashi, Y. (2012): *Damage of Rubber Bearings and Dampers of Bridges in 2011 Great East Japan Earthquake, Proceedings of the International Symposium on Engineering Lessons Learned from the 2011 Great East Japan Earthquake.*

[2] Japan Road Association (1996): *Specifications for Highway Bridges* Part 5 Seismic Design.

[3] Hata, Y., Takahashi, Y., Goto, H., Nozu, A. (2013): *Seismic Waveform Evaluation at Damage Sites of Rubber Bearings During the 2011 Off-Pacific Coast of Tohoku Earthquake Based on Records of Temporary Aftershock Observation, Journal of the Japan Association for Earthquake Engineering* 13 (3), pp. 30 – 56.

[4] Shinohara, S., Hoshikuma, J. (2014): *Experimental Research to Evaluate Characteristics of Earthquake-damaged Layered Rubber Bearing Containing Lead Plugs, Collection of Presented Papers to the 34th Workshop of the Japan Association of Earthquake Engineering, Japan Society of Civil Engineers.*

[5] Japan Road Association (2004): *Handbook for Road Bridge Bearings*.